

# THERMAL AND MASS STRATIFICATION EFFECTS ON UNSTEADY MHD PARABOLIC FLOW PAST AN INFINITE VERTICAL PLATE WITH VARIABLE TEMPERATURE AND MASS DIFFUSION THROUGH POROUS MEDIUM

 Pappu Das\*,  Rudra Kanta Deka

*Department of Mathematics, Gauhati University, Guwahati-781014, Assam, India*

*\*Corresponding Author e-mail: [pappudas751@gmail.com](mailto:pappudas751@gmail.com)*

Received March 03, 2024; revised April 15, 2024; accepted April 22, 2024

This study examines how thermal and mass stratification affect unsteady MHD parabolic flow past an infinite vertical plate through porous medium with variable heat and mass diffusion. Analytical solutions are derived for unitary Prandtl and Schmidt numbers using Laplace transform technique to simulate the flow's physical process. The investigation takes into account how the flow field is impacted by thermal and mass stratification. Following that, the outcomes of the stratification case are then compared with the scenario in which the flow field has no stratification. The finding of this study can help us comprehend more about the unsteady MHD parabolic flow and provide insightful information for stratified systems.

**Keywords:** *MHD flow; Vertical plate; Parabolic flow; Electrically conducting fluid; Unsteady flow; Stratified fluid; Porous medium*

**PACS:** 44.05.+e, 47.11.-j, 47.55.P-, 47.56.+r, 47.65.-d

## 1. INTRODUCTION

The most evident effect of thermal stratification is felt by anyone who has gone for a summer swim and felt the chilly water a few feet under the warm surface. The process by which density causes a body of fluid to develop comparatively stable and distinct layers is known as stratification of fluid which takes place mostly at higher temperatures. It happens mostly due to change in temperature, concentration, or the presence of various fluids with differing densities. Many natural systems, including lakes and oceans, exhibit the phenomenon of thermal stratification. Stratification obstructs the vertical fluid mixing that influences the exchange of nutrients, carbon, oxygen, and heat.

The study of parabolic flow problem plays an important role because it lessens viscous interactions between adjacent fluid layers and the pipe wall, which helps to minimize energy losses in flowing fluids. The parabolic motion has several uses, including solar cookers, solar concentrators, and parabolic trough solar collectors.

Using an infinite vertical plate in mass and heat transfer process is one of the applications for parabolic flow. Due to their significance in engineering and industrial processes such as the cooling of electronic equipment, sun collectors, solar cookers, solar concentrators, etc.—these difficulties are being studied in great detail. [1], [2], [3] and [4] came up with analytical solutions of different problems of thermal stratification or stratified fluid with various conditions. Numerous authors have been studied MHD flow past vertical plates and cylinders with stratification effects. [5], [6] and [7] studied MHD flow problems past vertical plate with stratification effects. [8] investigated the heat and mass diffusion flow along a surface in porous medium. [9] studied the effects of both thermal and mass stratification past an accelerated infinite vertical plate in porous medium. [10], conducted an investigation on parabolic flow problem past vertical plate, while [11] and [12] investigated MHD parabolic flow problems past vertical plates with several conditions.

In this article, we investigate the combined effects of thermal and mass stratification on unsteady MHD parabolic flow past an infinite vertical plate embedded in a porous medium with variable temperature and mass diffusion. For the unitary Prandtl and Schmidt numbers the solutions are then obtained. The investigation on velocity, temperature and concentration profiles are made under the impacts of variables and displayed on graphs. These variables include the thermal Grashof number  $Gr$ , mass Grashof number  $Gc$ , magnetic parameter  $M$ , time  $t$ , Darcy number  $Da$  and stratification parameters  $\gamma$  and  $\xi$ . On other physical phenomena including the rate of heat and mass transfer and skin friction, the effects of  $M$ ,  $Gr$ ,  $Gc$ ,  $\gamma$ ,  $\xi$  and  $t$  are also studied. For classical case when  $\gamma$  and  $\xi$  are absent, the solutions are then obtained and are compared to the original case that is when stratification is present. The conclusion of this study have numerous applications in engineering and several industries.

### 2. MATHEMATICAL ANALYSIS

In this work, we investigate an unstable MHD parabolic flow in two dimensions across an infinite vertical plate of a viscous, incompressible, and electrically conducting fluid embedded in a porous medium with variable temperature and mass diffusion. In order to examine the flow scenario, we utilize a coordinate system where the  $x'$  axis is selected vertically upward along the plate and the  $y'$  axis is perpendicular to the plate. The fluid and plate have the same initial fluid concentration  $C'_\infty$  and starting temperature  $T'_\infty$ . The plate is moving with the velocity  $U_R t'^2$  in its own plane at time  $t' > 0$  relative to the gravitational field. Also the plate temperature and concentration level are raised to  $T'_w$  and  $C'_w$  respectively at time  $t' > 0$ . Due to the infinite length of the plate, all the flow variables are independent of  $x'$  and only impacted by  $y'$  and  $t'$ . The equations for motion, energy, and concentration are then represented by the Boussinesq's approximation as follows:

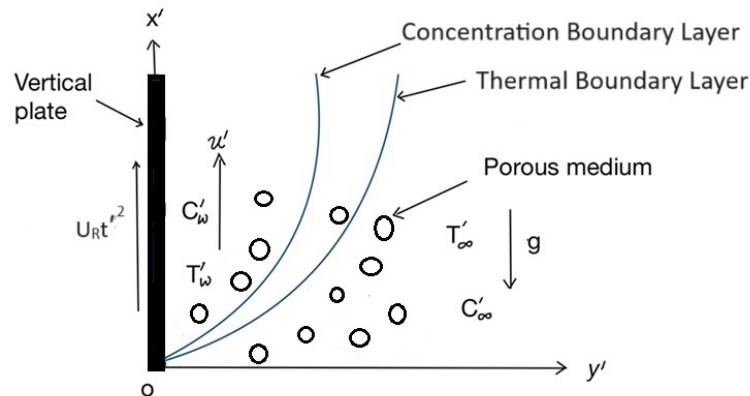


Figure 1. Physical model of the problem

$$\frac{\partial u'}{\partial t'} = \nu \frac{\partial^2 u'}{\partial y'^2} + [g\beta(T' - T'_\infty) + g\beta_c(C' - C'_\infty)] - \frac{\sigma B_0^2 u'}{\rho} - \frac{\nu u'}{k'} \tag{1}$$

$$\frac{\partial T'}{\partial t'} = \frac{k}{\rho C_p} \frac{\partial^2 T'}{\partial y'^2} - \gamma' u' \tag{2}$$

$$\frac{\partial C'}{\partial t'} = D \frac{\partial^2 C'}{\partial y'^2} - \xi' u' \tag{3}$$

Considering the initial and boundary conditions as:

$$u' = 0, \quad T' = T'_\infty, \quad C' = C'_\infty \quad \forall y', t' \leq 0$$

$$u' = U_R t'^2, \quad T' = T'_\infty + (T'_w - T'_\infty) A t',$$

$$C' = C'_\infty + (C'_w - C'_\infty) A t' \quad \text{at } y' = 0, \quad t' > 0 \tag{4}$$

$$u' \rightarrow 0, \quad T' \rightarrow T'_\infty, \quad C' \rightarrow C'_\infty \quad \text{as } y' \rightarrow \infty, \quad t' > 0$$

where,  $\gamma' = \frac{dT'_\infty}{dx'} + \frac{g}{C_p}$  denotes the thermal stratification parameter and  $\frac{dT'_\infty}{dx'}$  denotes the vertical temperature convection known as thermal stratification. In addition,  $\frac{g}{C_p}$  represents the rate of reversible work done on fluid particles by compression, often known as work of compression. The variable ( $\gamma'$ ) denotes the thermal stratification parameter in our study as the compression work is relatively minimal. Regarding testing of computational methods, compression work is kept as an additive to thermal stratification.

Now, we introduce the following non-dimensional quantities:

$$\begin{aligned}
 y &= \frac{y'}{L_R}, \quad t = \frac{t'}{t_R}, \quad u = \frac{u'}{U_R}, \quad Da = \frac{U_R^2 k'}{\nu^2}, \quad , \quad Pr = \frac{\mu C_p}{k} \\
 M &= \frac{\sigma B_0^2 \nu}{\rho U_R^2}, \quad Sc = \frac{\nu}{D}, \quad \theta = \frac{T' - T'_\infty}{T'_w - T'_\infty}, \quad C = \frac{C' - C'_\infty}{C'_w - C'_\infty}, \quad \Delta T = T'_w - T'_\infty \tag{5} \\
 Gc &= \frac{\nu g \beta_c (C'_w - C'_\infty)}{U_R^3}, \quad U_R = (\nu g \beta \Delta T)^{1/3}, \quad L_R = \left( \frac{g \beta \Delta T}{\nu^2} \right)^{-1/3}, \quad A = \frac{1}{t_R}, \\
 t_R &= (g \beta \Delta T)^{-2/3} \nu^{1/3}, \quad Gr = \frac{\nu g \beta (T'_w - T'_\infty)}{U_R^3}, \quad \gamma = \frac{\gamma' L_R}{\Delta T}, \quad \xi = \frac{\xi' L_R}{C' - C'_\infty}
 \end{aligned}$$

When the non-dimensional quantities defined in (5) above are employed, equations (1), (2), and (3) take on the following forms:

$$\frac{\partial u}{\partial t} = \frac{\partial^2 u}{\partial y^2} + Gr\theta + GcC - \left( M + \frac{1}{Da} \right) u \tag{6}$$

$$\frac{\partial \theta}{\partial t} = \frac{1}{Pr} \frac{\partial^2 \theta}{\partial y^2} - \gamma u \tag{7}$$

$$\frac{\partial C}{\partial t} = \frac{1}{Sc} \frac{\partial^2 C}{\partial y^2} - \xi u \tag{8}$$

And the corresponding initial and boundary conditions (4) then reduce to,

$$u = 0, \quad \theta = 0, \quad C = 0 \quad \forall y, t \leq 0$$

$$u = t^2, \quad \theta = t, \quad C = t \quad \text{at } y = 0, t > 0 \tag{9}$$

$$u \rightarrow 0, \quad \theta \rightarrow 0, \quad C \rightarrow 0 \quad \text{as } y \rightarrow \infty, t > 0$$

### 2.1. Method of Solution

Solving the non-dimensional governing equations (6), (7) and (8) with respect to the boundary conditions (9) for the unitary Prandtl and Schmidt numbers, we obtain the velocity, temperature and concentration profiles with the help of [13] and [14] as:

$$u = C_1 f(A_1) - C_2 [h(A_1) - h(B_1)] - C_3 f(B_1) \tag{10}$$

$$\theta = t D_1 \left[ \left( 1 + \frac{y^2}{2t} \right) \operatorname{erfc} \left( \frac{y}{2\sqrt{t}} \right) - \frac{y e^{-\frac{y^2}{4t}}}{\sqrt{\pi t}} \right] + D_2 [f(A_1) - f(B_1)] + D_3 h(B_1) - D_4 h(A_1) \tag{11}$$

$$C = t E_1 \left[ \left( 1 + \frac{y^2}{2t} \right) \operatorname{erfc} \left( \frac{y}{2\sqrt{t}} \right) - \frac{y e^{-\frac{y^2}{4t}}}{\sqrt{\pi t}} \right] + E_2 [f(A_1) - f(B_1)] + E_3 h(B_1) - E_4 h(A_1) \tag{12}$$

For the sake of succinctness, our study refers to the situation where pressure work is omitted and the environment is isothermal ( $\gamma = 0, \xi = 0$ ) as the classical scenario. The velocity ( $u^*$ ), temperature ( $\theta^*$ ) and concentration ( $C^*$ ) profiles for classical case are obtained as,

$$u^* = f(N) - F_1 h(N) + F_1 \left[ \left( 1 + \frac{y^2}{2t} \right) \operatorname{erfc} \left( \frac{y}{2\sqrt{t}} \right) - \frac{ye^{-\frac{y^2}{4t}}}{\sqrt{\pi t}} \right] \tag{13}$$

$$\theta^* = t \left[ \left( 1 + \frac{y^2}{2t} \right) \operatorname{erfc} \left( \frac{y}{2\sqrt{t}} \right) - \frac{ye^{-\frac{y^2}{4t}}}{\sqrt{\pi t}} \right] \tag{14}$$

$$C^* = t \left[ \left( 1 + \frac{y^2}{2t} \right) \operatorname{erfc} \left( \frac{y}{2\sqrt{t}} \right) - \frac{ye^{-\frac{y^2}{4t}}}{\sqrt{\pi t}} \right] \tag{15}$$

where

$$\begin{aligned} N &= M + \frac{1}{Da}, \quad A_1 = \frac{N + \sqrt{N^2 - 4\gamma Gr - 4\xi Gc}}{2}, \quad B_1 = \frac{N - \sqrt{N^2 - 4\gamma Gr - 4\xi Gc}}{2}, \quad C_1 = \frac{A_1}{A_1 - B_1}, \\ C_2 &= \frac{Gr + Gc}{A_1 - B_1}, \quad C_3 = \frac{B_1}{A_1 - B_1}, \quad D_1 = 1 - \frac{\gamma(Gr + Gc)}{A_1 B_1}, \quad D_2 = \frac{\gamma}{A_1 - B_1}, \quad D_3 = \frac{\gamma(Gr + Gc)}{B_1(A_1 - B_1)}, \\ D_4 &= \frac{\gamma(Gr + Gc)}{A_1(A_1 - B_1)}, \quad E_1 = 1 - \frac{\xi(Gr + Gc)}{A_1 B_1}, \quad E_2 = \frac{\xi}{A_1 - B_1}, \quad E_3 = \frac{\xi(Gr + Gc)}{B_1(A_1 - B_1)}, \quad E_4 = \frac{\xi(Gr + Gc)}{A_1(A_1 - B_1)}, \quad F_1 = \frac{Gr + Gc}{N}. \end{aligned}$$

And  $f$  and  $h$  are inverse Laplace transforms and are given by

$$f(A_1) = L^{-1} \left\{ \frac{e^{-y\sqrt{s+A_1}}}{s^3} \right\} \text{ and } h(A_1) = L^{-1} \left\{ \frac{e^{-y\sqrt{s+A_1}}}{s^2} \right\}$$

Using the formulas given by [14], we separate the complex arguments of the error function that were present in the preceding expressions into real and imaginary components.

### 2.2. Skin-Friction

The non-dimensional computation of skin-friction of the plate is given by:

$$\tau = - \left. \frac{du}{dy} \right|_{y=0} \tag{16}$$

Now from equation (10) we get the expression for skin-friction as,

$$\begin{aligned} \tau &= \frac{C_1}{2} \left[ t^2 \sqrt{A} \operatorname{erf}(\sqrt{At}) + \sqrt{\frac{t}{\pi}} t e^{-At} - \frac{\operatorname{erf}(\sqrt{At})}{4A^{\frac{3}{2}}} + \frac{\operatorname{terf}(\sqrt{At})}{\sqrt{A}} + \frac{\sqrt{t} e^{-At}}{2A\sqrt{\pi}} \right] - \frac{C_3}{2} \left[ t^2 \sqrt{B} \operatorname{erf}(\sqrt{Bt}) + \sqrt{\frac{t}{\pi}} t e^{-Bt} \right. \\ &- \frac{\operatorname{erf}(\sqrt{Bt})}{4B^{\frac{3}{2}}} + \frac{\operatorname{terf}(\sqrt{Bt})}{\sqrt{B}} + \left. \frac{\sqrt{t} e^{-Bt}}{2B\sqrt{\pi}} \right] - C_2 \left[ t \sqrt{A} \operatorname{erf}(\sqrt{At}) + \sqrt{\frac{t}{\pi}} e^{-At} + \frac{\operatorname{erf}(\sqrt{At})}{2\sqrt{A}} - t \sqrt{B} \operatorname{erf}(\sqrt{Bt}) + \sqrt{\frac{t}{\pi}} e^{-Bt} \right. \\ &\left. + \frac{\operatorname{erf}(\sqrt{Bt})}{2\sqrt{B}} \right] \tag{17} \end{aligned}$$

Skin-friction in classical scenario is obtained as,

$$\begin{aligned} \tau^* &= \frac{1}{2} \left[ t^2 \sqrt{N} \operatorname{erf}(\sqrt{Nt}) + \sqrt{\frac{t}{\pi}} t e^{-Nt} - \left( \frac{1}{4N} - t \right) \frac{\operatorname{erf}(\sqrt{Nt})}{\sqrt{N}} + \sqrt{\frac{t}{\pi}} \frac{e^{-Nt}}{2N} \right] - \frac{Gr + Gc}{N} \left[ t \sqrt{N} \operatorname{erf}(\sqrt{Nt}) + \right. \\ &\left. \sqrt{\frac{t}{\pi}} (2 + e^{-Nt}) + \frac{\operatorname{erf}(\sqrt{Nt})}{\sqrt{N}} \right] \tag{18} \end{aligned}$$

### 2.3. Plate Heat Flux (Nusselt Number)

The non-dimensional form of rate of heat transfer (Nusselt Number) is given by,

$$Nu = -\frac{d\theta}{dy}\Big|_{y=0} \tag{19}$$

Now from equation (11) we get the expression for Nusselt number as,

$$Nu = 2D_1\sqrt{\frac{t}{\pi}} + \frac{D_2}{2} \left[ t^2\sqrt{A}erf(\sqrt{At}) + \sqrt{\frac{t}{\pi}}te^{-At} - \frac{erf(\sqrt{At})}{4A^{\frac{3}{2}}} + \frac{terf(\sqrt{At})}{\sqrt{A}} + \frac{\sqrt{t}e^{-At}}{2A\sqrt{\pi}} - t^2\sqrt{B}erf(\sqrt{Bt}) - \sqrt{\frac{t}{\pi}}te^{-Bt} + \frac{erf(\sqrt{Bt})}{4B^{\frac{3}{2}}} - \frac{terf(\sqrt{Bt})}{\sqrt{B}} - \frac{\sqrt{t}e^{-Bt}}{2B\sqrt{\pi}} \right] - D_4 \left[ t\sqrt{A}erf(\sqrt{At}) + \sqrt{\frac{t}{\pi}}e^{-At} + \frac{erf(\sqrt{At})}{2\sqrt{A}} \right] + D_3 \left[ t\sqrt{B}erf(\sqrt{Bt}) + \sqrt{\frac{t}{\pi}}e^{-Bt} + \frac{erf(\sqrt{Bt})}{2\sqrt{B}} \right] \tag{20}$$

For classical case, Nusselt number is derived as,

$$Nu^* = 2\sqrt{\frac{t}{\pi}} \tag{21}$$

### 2.4. Sherwood Number

The non-dimensional form of rate of mass transfer (Sherwood Number) is given by,

$$Sh = -\frac{dC}{dy}\Big|_{y=0} \tag{22}$$

Now from equation (12) we get the expression for Sherwood number as,

$$Sh = 2E_1\sqrt{\frac{t}{\pi}} + \frac{E_2}{2} \left[ t^2\sqrt{A}erf(\sqrt{At}) + \sqrt{\frac{t}{\pi}}te^{-At} - \frac{erf(\sqrt{At})}{4A^{\frac{3}{2}}} + \frac{terf(\sqrt{At})}{\sqrt{A}} + \frac{\sqrt{t}e^{-At}}{2A\sqrt{\pi}} - t^2\sqrt{B}erf(\sqrt{Bt}) - \sqrt{\frac{t}{\pi}}te^{-Bt} + \frac{erf(\sqrt{Bt})}{4B^{\frac{3}{2}}} - \frac{terf(\sqrt{Bt})}{\sqrt{B}} - \frac{\sqrt{t}e^{-Bt}}{2B\sqrt{\pi}} \right] - E_4 \left[ t\sqrt{A}erf(\sqrt{At}) + \sqrt{\frac{t}{\pi}}e^{-At} + \frac{erf(\sqrt{At})}{2\sqrt{A}} \right] + E_3 \left[ t\sqrt{B}erf(\sqrt{Bt}) + \sqrt{\frac{t}{\pi}}e^{-Bt} + \frac{erf(\sqrt{Bt})}{2\sqrt{B}} \right] \tag{23}$$

For classical case, Sherwood number is obtained as,

$$Sh^* = 2\sqrt{\frac{t}{\pi}} \tag{24}$$

## 3. RESULTS AND DISCUSSIONS

The solutions obtained from the previous section’s numerical computations are displayed in Figures from 2 to 25 and discuss the effects of various physical parameters on temperature, velocity, concentration fields, skin friction, Nusselt number, and Sherwood number, which provides us with better insight of the problem in terms of physical significance. It has been found that a stratified fluid moves slower in compare to unstratified fluid because of density varying property a resistive type of force (Lorentz force) occurs which lowers the flow velocity. The velocity profiles are shown in figures from 2 to 7 for different values of magnetic parameter  $M$ ,

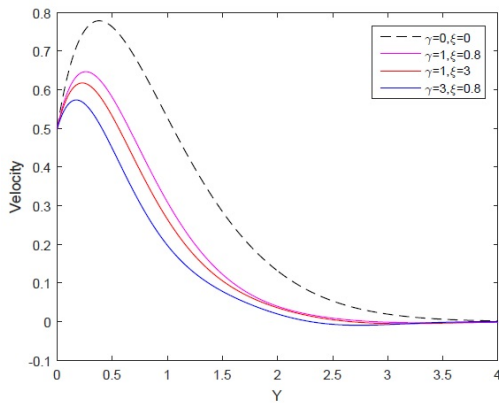


**Figure 2.** Effects of  $\gamma$  and  $\xi$  on Velocity Profile for  $Gr = 5, Gc = 5, t = 1, M = 1, Da = 0.5$

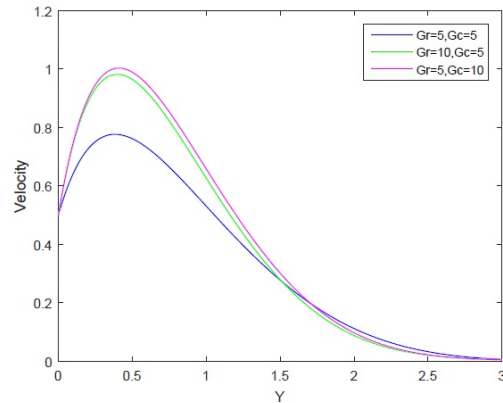


**Figure 3.** Effects of  $Gr$  and  $Gc$  on Velocity Profile for  $\gamma = 1, \xi = 0.8, t = 1, M = 1, Da = 0.5$

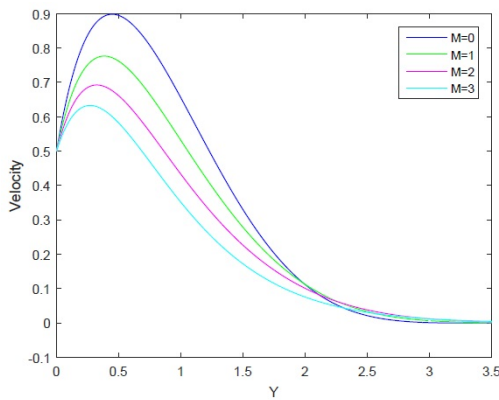


**Figure 4.** Effects of  $M$  on Velocity Profile for  $\gamma = 1, \xi = 0.8, Gr = 5, Gc = 5, t = 1, Da = 0.5$

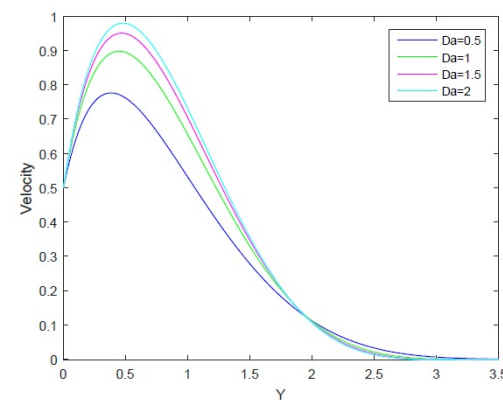


**Figure 5.** Effects of  $Da$  on Velocity Profile for  $\gamma = 1, \xi = 0.8, Gr = 5, Gc = 5, M = 1, t = 1$

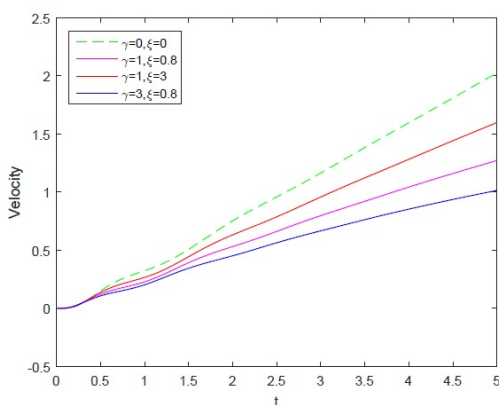


**Figure 6.** Effects of  $\gamma$  and  $\xi$  on Velocity Profile against time for  $y = 1, Gr = 5, Gc = 5, M = 1, Da = 0.5$

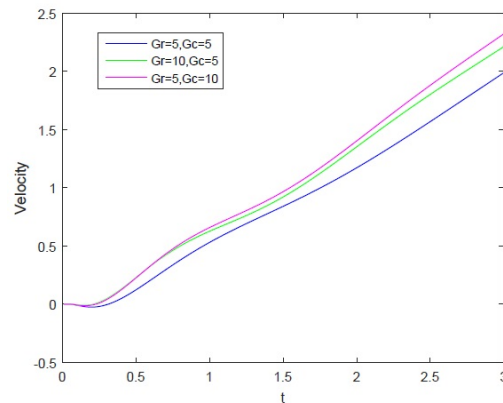


**Figure 7.** Effects of  $Gr$  and  $Gc$  on Velocity Profile against time for  $y = 1, \gamma = 1, \xi = 0.8, M = 1, Da = 0.5$

Darcy number  $Da$ , thermal Grashof number  $Gr$ , mass Grashof number  $Gc$ , thermal stratification parameter  $\gamma$ , mass stratification parameter  $\xi$  and time  $t$ . As the values of  $\gamma$  and  $\xi$ , which stand for thermal and mass stratification, rise, the velocity decreases. It has been observed that when the magnetic parameter  $M$  increases, the velocity profile falls because the flow velocity is lowered due to a resistive type of force known as the Lorentz force occurs. When thermal Grashof number  $Gr$ , mass Grashof number  $Gc$ , and Darcy number  $Da$  increase, velocity profile and velocity profile against time increase as well in both classical and non-classical cases. The velocity profile against time increases in classical ( $\gamma = 0$  and  $\xi = 0$ ) case in compare to the stratified case.

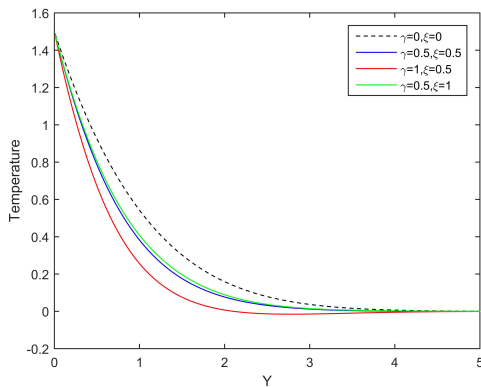


**Figure 8.** Effects of  $\gamma$  and  $\xi$  on Temperature Profile for  $Gr = 5, Gc = 5, t = 1.5, M = 1, Da = 0.5$

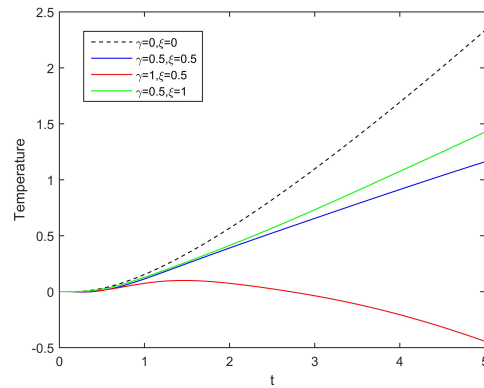


**Figure 9.** Effects of  $\gamma$  and  $\xi$  on Temperature Profile against time for  $y = 1.5, Gr = 5, Gc = 5, M = 1, Da = 0.5$

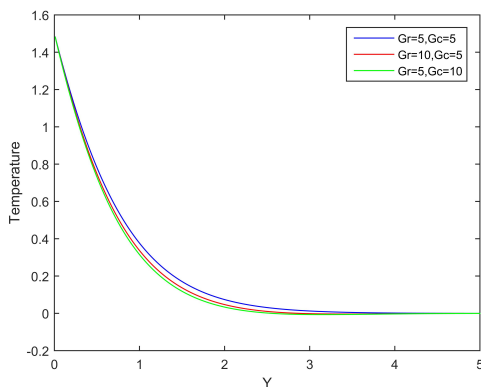


**Figure 10.** Effects of  $Gr$  and  $Gc$  on Temperature Profile for  $\gamma = 1, \xi = 0.8, t = 1.5, M = 1, Da = 0.5$

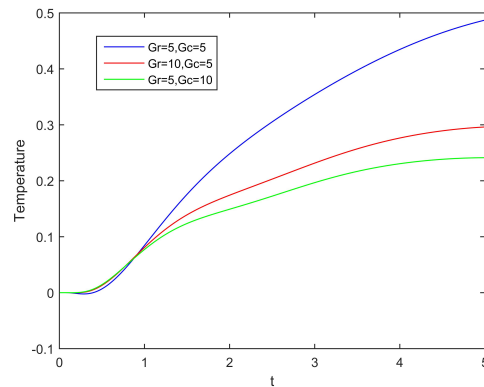


**Figure 11.** Effects of  $Gr$  and  $Gc$  on Temperature Profile against time for  $y = 1.5, \gamma = 1, \xi = 0.8, M = 1, Da = 0.5$

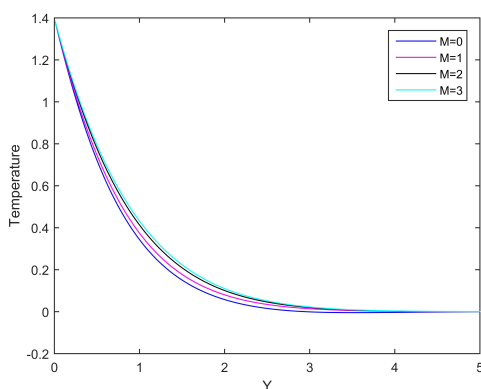


**Figure 12.** Effects of  $M$  on Temperature Profile for  $\gamma = 1, \xi = 0.8, Gr = 5, Gc = 5, t = 1.5, Da = 0.5$

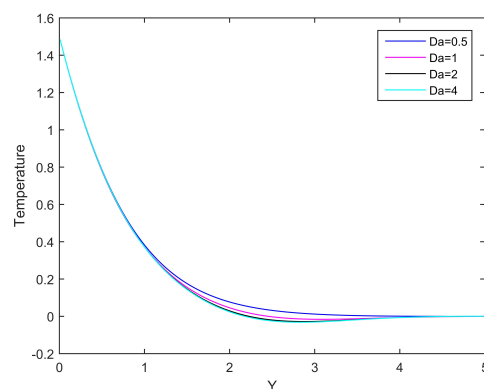


**Figure 13.** Effects of  $Da$  on Temperature Profile for  $\gamma = 1, \xi = 0.8, Gr = 5, Gc = 5, t = 1.5, M = 1$

The temperature and concentration profiles with and without stratification for various values of  $\gamma, \xi, M, Gr, Gc, Da$  and  $t$  are shown graphically in figures 8 to 19. From figures 8 and 9 it is seen that temperature is more in classical case as compared to the non-classical case. Likewise figures 14 and 15 depict that concentration is less in stratified fluid in compare to the unstratified fluid. Figures 12 and 18 depict the effect of magnetic parameter  $M$  on temperature and concentration profile. Temperature and concentration increase as  $M$  increases. From figures 13 and 19 it is seen that as Darcy number ( $Da$ ) grows, temperature and concentration fall down.

It is clear from figures 10 and 11 and 16 and 17 that temperature and concentration decrease when the thermal and mass Grashof numbers ( $Gr$  and  $Gc$ ) increase.

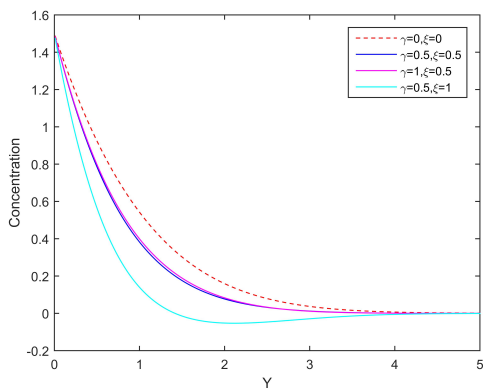


**Figure 14.** Effects of  $\gamma$  and  $\xi$  on Concentration Profile for  $Gr = 5, Gc = 5, t = 1.5, M = 1, Da = 0.5$

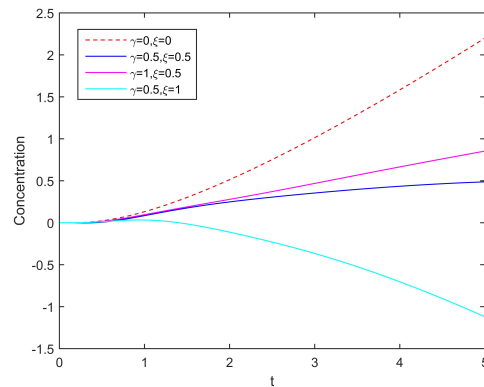


**Figure 15.** Effects of  $\gamma$  and  $\xi$  on Concentration Profile against time for  $y = 1.5, Gr = 5, Gc = 5, M = 1, Da = 0.5$

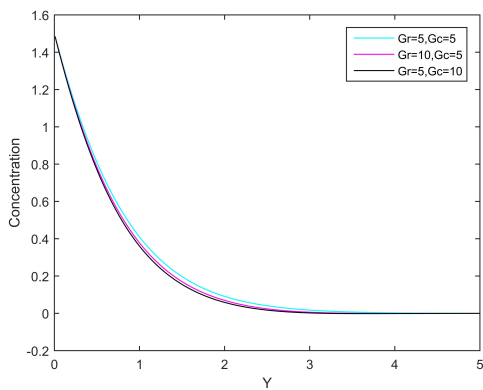


**Figure 16.** Effects of  $Gr$  and  $Gc$  on Concentration Profile for  $\gamma = 1, \xi = 0.8, t = 1.5, M = 1, Da = 0.5$

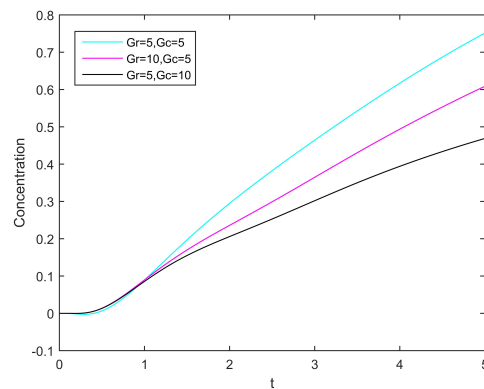


**Figure 17.** Effects of  $Gr$  and  $Gc$  on Concentration Profile against time for  $y = 1.5, \gamma = 1, \xi = 0.8, M = 1, Da = 0.5$

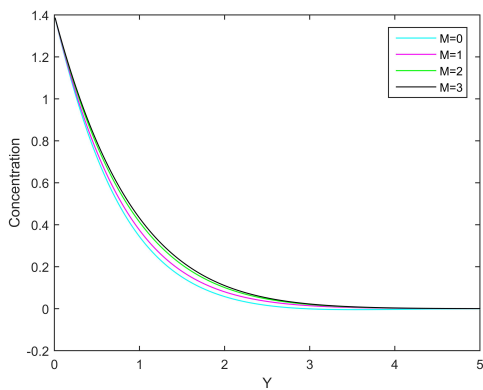


**Figure 18.** Effects of  $M$  on Concentration Profile for  $\gamma = 1, \xi = 0.8, Gr = 5, Gc = 5, t = 1.5, Da = 0.5$

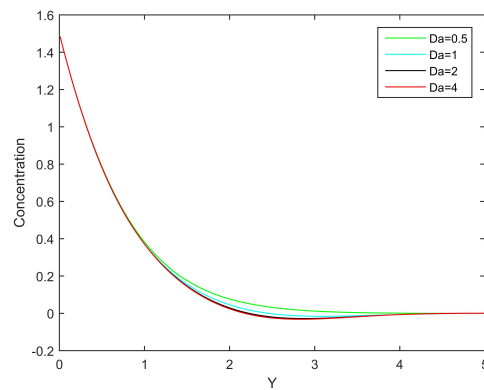


**Figure 19.** Effects of  $Da$  on Concentration Profile for  $\gamma = 1, \xi = 0.8, Gr = 5, Gc = 5, t = 1.5, M = 1$

The effects of  $\gamma, \xi$ , thermal Grashof ( $Gr$ ) and mass Grashof ( $Gc$ ) numbers on skin-friction, Nusselt number and Sherwood number are presented in the figures 20 to 25. In classical case that is when  $\gamma = 0$  and  $\xi = 0$ ,



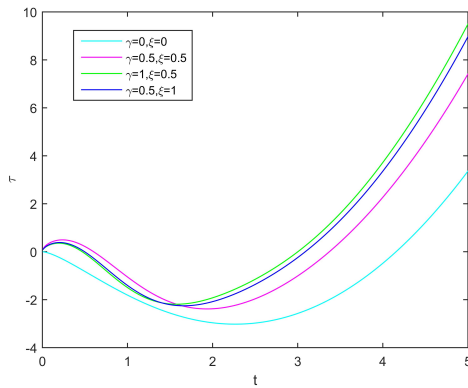


**Figure 20.** Effects of  $\gamma$  and  $\xi$  on skin-friction for  $Gr = 5, Gc = 5, M = 1, Da = 0.5$

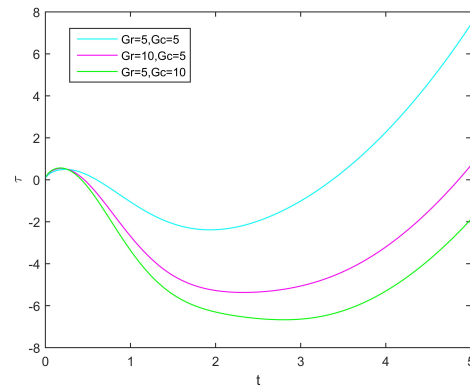


**Figure 21.** Effects of  $Gr$  and  $Gc$  on skin-friction for  $\gamma = 1, \xi = 0.8, M = 1, Da = 0.5$

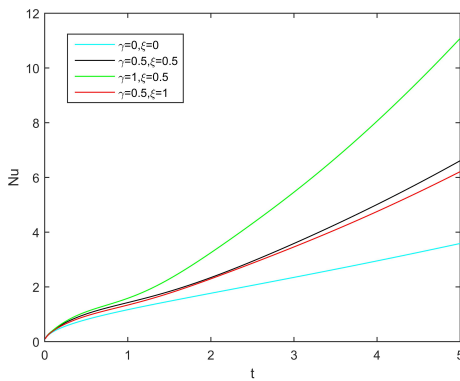


**Figure 22.** Effects of  $\gamma$  and  $\xi$  on Nusselt number for  $Gr = 5, Gc = 5, M = 1, Da = 0.5$

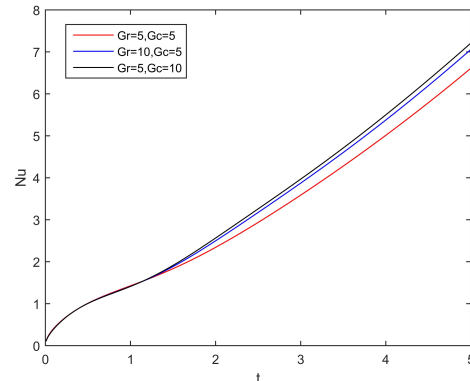


**Figure 23.** Effects of  $Gr$  and  $Gc$  on Nusselt number for  $\gamma = 1, \xi = 0.8, M = 1, Da = 0.5$

skin-friction, Nusselt number and Sherwood number decrease as compared to the stratification case. It has been observed that while rising in the values of  $Gr$  and  $Gc$ , skin-friction falls down. In case of Nusselt and Sherwood numbers, when  $Gr$  and  $Gc$  increase, both Nusselt and Sherwood numbers increase.

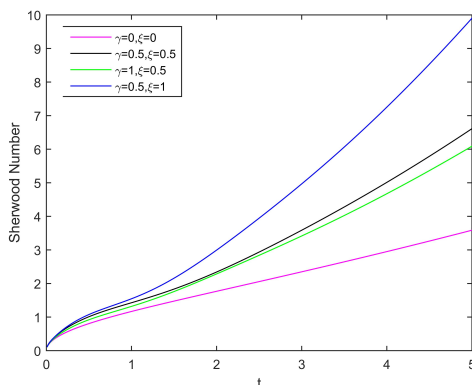


**Figure 24.** Effects of  $\gamma$  and  $\xi$  on Sherwood number for  $Gr = 5, Gc = 5, M = 1, Da = 0.5$

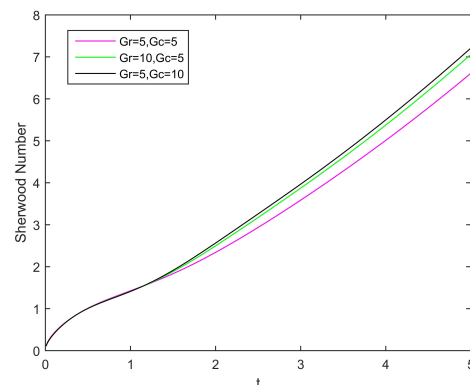


**Figure 25.** Effects of  $Gr$  and  $Gc$  on Sherwood number for  $\gamma = 1, \xi = 0.8, M = 1, Da = 0.5$


#### 4. CONCLUSION

We have explored the impact of thermal and mass stratification on unsteady MHD parabolic flow past an infinite vertical plate embedded in a porous medium with variable heat and mass diffusion. The present

study's findings have been juxtaposed with those of the classical scenario in which stratification is absent. The conclusion of our study that based on the results derived from the previous sections are as follows:

- When  $\gamma$  and  $\xi$  grow, velocity, temperature and concentration drop as both the stratification (thermal and mass) effect stabilises the fluid and becomes steady state. But in the classical situation, velocity, temperature and concentration are higher than in the thermally and mass stratified fluid.
- Velocity, temperature and concentration profiles grow as  $Gr$  and  $Gc$  increase but velocity decreases as  $M$  increases and both temperature and concentration rise as  $M$  grows.
- Velocity grows as Darcy number  $Da$  increases but temperature and concentration fall down as  $Da$  rises.
- Skin-friction, Nusselt number and Sherwood number decrease in isothermal case as compared to the stratification case.
- With rising the values of  $Gr$  and  $Gc$ , Nusselt number and Sherwood number also increase but skin-friction falls down.

#### ORCID

 Pappu Das, <https://orcid.org/0009-0007-8006-3659>;  Rudra Kanta Deka, <https://orcid.org/0009-0007-1573-4890>

#### REFERENCES

- [1] J.S. Park, and J.M. Hyun, "Transient behavior of vertical buoyancy layer in a stratified fluid," *Intl. J. Heat Mass Transfer*, **41**, 4393-4397 (1998). [https://doi.org/10.1016/S0017-9310\(98\)00175-6](https://doi.org/10.1016/S0017-9310(98)00175-6)
- [2] J.S. Park, "Transient buoyant flows of a stratified fluid in a vertical channel," *KSME. Intl. J.* **15**, 656-664 (2001). <https://doi.org/10.1007/BF03184382>
- [3] A. Shapiro, and E. Fedorovich, "Unsteady convectively driven flow along a vertical plate immersed in a stably stratified fluid," *J. Fluid Mech.* **498**, 333-352 (2004). <https://doi.org/10.1017/S0022112003006803>
- [4] E. Magyari, I. Pop, and B. Keller, "Unsteady free convection along an infinite vertical flat plate embedded in a stably stratified fluid-saturated porous medium," *Transport in Porous Media*, **62**, 233-249 (2006). <https://doi.org/10.1007/s11242-005-1292-6>
- [5] B.C. Neog, and R.K. Deka, "Unsteady natural convection flow past an accelerated vertical plate in a thermally stratified fluid," *Theoret. Appl. Mech.* **36**(4), 261-274 (2009). <https://doi.org/10.2298/TAM0904261D>
- [6] R.K. Deka, and A. Bhattacharya, "Magneto-Hydrodynamic (MHD) flow past an infinite vertical plate immersed in a stably stratified fluid," *International Journal of the Physical Sciences*, **6**(24), 5831-5836 (2011). <https://doi.org/10.5897/IJPS11.011>
- [7] S. Gurminder, P.R. Sharma, and A.J. Chamkha, "Effect of thermally stratified ambient fluid on MHD convective flow along a moving non isothermal vertical plate," *Intl. J. Phy. Sci.* **5**(3), 208-215 (2010). <https://doi.org/10.5897/IJPS.9000199>
- [8] R.C. Chaudhary, and A. Jain, "MHD heat and mass diffusion flow by natural convection past a surface embedded in a porous medium," *Theoret. Appl. Mech.* **36**(1), 1-27 (2009). <http://dx.doi.org/10.2298/TAM0901001C>
- [9] H. Kumar, and R.K. Deka, "Thermal and mass stratification effects on unsteady flow past an accelerated infinite vertical plate with variable temperature and exponential mass diffusion in porous medium," *East European Journal of Physics*, (4), 87-97 (2023). <https://doi.org/10.26565/2312-4334-2023-4-09>
- [10] R.S. Nath, R.K. Deka, and H. Kumar, "The Effect of Thermal Stratification on Unsteady Parabolic Flow past an Infinite Vertical Plate with Chemical Reaction," *East European Journal of Physics*, (4), 77-86 (2023). <https://doi.org/10.26565/2312-4334-2023-4-08>
- [11] A. Selvaraj, S.D. Jose, R. Muthucumaraswamy, and S. Karthikeyan, "MHD-parabolic flow past an accelerated isothermal vertical plate with heat and mass diffusion in the presence of rotation," *Materials Today: Proceedings*, **46**, 3546-3549 (2021). <https://doi.org/10.1016/j.matpr.2020.12.499>
- [12] R. Muthucumaraswamy, and P. Sivakumar, "Hydromagnetic effects on parabolic flow past an infinite vertical plate with variable mass diffusion in the presence of thermal radiation and chemical reaction," *ARPN Journal of Engineering and Applied Sciences*, **10**(12) (2015). <http://dx.doi.org/10.13140/RG.2.2.13011.84008>
- [13] R.B. Hetnarski, "An algorithm for generating some inverse laplace transforms of exponential form," *Zeitschrift fur angewandte Mathematik und Physik ZAMP*, **26**, 249-253 (1975). <https://doi.org/10.1007/BF01591514>
- [14] M. Abramowitz, I.A. Stegun, and R.H. Romer. "Handbook of mathematical functions with formulas, graphs, and mathematical tables," *American Journal of Physics*, **56**(10), 958 (1988). <https://doi.org/10.1119/1.15378>

**ВПЛИВ ТЕРМІЧНОЇ ТА МАСОВОЇ СТРАТИФІКАЦІЇ НА НЕСТАЦІОНАРНИЙ  
МГД-ПАРАБОЛІЧНИЙ ПОТІК ПОВЗ НЕСКІНЧЕННУ ВЕРТИКАЛЬНУ ПЛАСТИНУ  
ЗІ ЗМІННОЮ ТЕМПЕРАТУРОЮ ТА ДИФУЗИЄЮ МАСИ ЧЕРЕЗ  
ПОРИСТЕ СЕРЕДОВИЩЕ**

**Паппу Дас, Рудра Канта Дека**

*Факультет математики, Університет Гаухаті, Гуваяті-781014, Ассам, Індія*

У цьому дослідженні досліджується, як теплова та масова стратифікація впливає на нестационарний МГД-параболічний потік повз нескінченну вертикальну пластину через пористе середовище зі змінною дифузійною теплою та масою. Аналітичні рішення отримані для унітарних чисел Прандтля та Шмідта з використанням техніки перетворення Лапласа для моделювання фізичного процесу потоку. Дослідження бере до уваги те, як на поле течії впливає теплова та масова стратифікація. Після цього результати випадку стратифікації порівнюються зі сценарієм, у якому поле потоку не має стратифікації. Результати цього дослідження можуть допомогти нам зрозуміти більше про нестационарний МГД-параболічний потік і надати глибоку інформацію для стратифікованих систем.

**Ключові слова:** МГД потік; вертикальна пластину; параболічний потік; електропровідна рідина; нестабільний потік; стратифікована рідина; пористе середовище